Annals of Clinical and Translational Neurology

RESEARCH ARTICLE OPEN ACCESS

Cervical Spinal Cord Magnetization Transfer Ratio and Its Relationship With Clinical Outcomes in Multiple Sclerosis

Lisa Eunyoung Lee[1,2,3] | Julien Cohen-Adad[4,5,6] | Irene M. Vavasour[7] | Melanie Guenette[2] | Katherine Sawicka[1,8,9] | Neda Rashidi-Ranjbar[3] | Nathan Churchill[3,10] | Akash Chopra[11] | Adelia Adelia[11] | Pierre-Louis Benveniste[4,6] | Anthony Traboulsee[11] | Nathalie Arbour[12] | Fabrizio Giuliani[13] | Larry D. Lynd[14,15] | Scott B. Patten[16] | Alexandre Prat[12] | Alice Schabas[11] | Penelope Smyth[13] | Roger Tam[7,17] | Yunyan Zhang[18] | Simon J. Graham[19] | Mojgan Hodaie[20] | Anthony Feinstein[21] | Shannon Kolind[7,11,22] | Tom A. Schweizer[1,3,20] | Jiwon Oh[1,2,3] | CanProCo Study Group

[1]Department of Medicine (Neurology), University of Toronto, Toronto, Ontario, Canada | [2]BARLO Multiple Sclerosis Centre, St. Michael's Hospital, Unity Health Toronto, Toronto, Ontario, Canada | [3]Keenan Research Centre, St. Michael's Hospital, Unity Health Toronto, Toronto, Ontario, Canada | [4]NeuroPoly Lab, Institute of Biomedical Engineering, Polytechnique Montréal, Montreal, QC, Canada | [5]Functional Neuroimaging Unit, CRIUGM, Montreal, QC, Canada | [6]Mila-Quebec AI Institute, Montreal, QC, Canada | [7]Department of Radiology, University of British Columbia, Vancouver, B.C., Canada | [8]Dalla Lana School of Public Health, Institute of Health Policy, Management and Evaluation, University of Toronto, Toronto, Ontario, Canada | [9]Child Health Evaluative Sciences Program, SickKids Research Institute, Toronto, Ontario, Canada | [10]Department of Physics, Toronto Metropolitan University, Toronto, Ontario, Canada | [11]Department of Medicine (Neurology), University of British Columbia, Vancouver, B.C., Canada | [12]Department of Neurosciences, Faculty of Medicine, Université de Montréal and Centre Hospitalier de l'Université de Montréal, Montreal, QC, Canada | [13]Department of Medicine (Neurology) and Neurosciences and Mental Health Institute, University of Alberta, Edmonton, Alberta, Canada | [14]Faculty of Pharmaceutical Sciences, University of British Columbia, Vancouver, B.C., Canada | [15]Centre for Advancing Health Outcomes, Providence Health Research Institute, Vancouver, B.C., Canada | [16]Department of Community Health Sciences, University of Calgary, Calgary, Alberta, Canada | [17]School of Biomedical Engineering, University of British Columbia, Vancouver, B.C., Canada | [18]Departments of Radiology & Clinical Neurosciences, University of Calgary, Calgary, Alberta, Canada | [19]Department of Medical Biophysics, University of Toronto, Toronto, Ontario, Canada | [20]Department of Surgery, University of Toronto, Toronto, Ontario, Canada | [21]Department of Psychiatry, University of Toronto, Toronto, Ontario, Canada | [22]Department of Physics and Astronomy, University of British Columbia, Vancouver, B.C., Canada

Correspondence: Jiwon Oh (jiwon.oh@unityhealth.to)

Received: 7 February 2025 | **Revised:** 12 May 2025 | **Accepted:** 3 June 2025

Funding: This work was supported by F. Hoffmann-La Roche. Fondation Brain Canada. Multiple Sclerosis Canada. Government of Alberta. Biogen.

Keywords: MRI | multiple sclerosis | spinal cord

ABSTRACT

Objective: The cervical spinal cord (cSC) is highly relevant to clinical dysfunction in multiple sclerosis (MS) but remains understudied using quantitative magnetic resonance imaging (MRI). We assessed magnetization transfer ratio (MTR), a semi-quantitative MRI measure sensitive to MS-related tissue microstructural changes, in the cSC and its relationship with clinical outcomes in radiologically isolated syndrome (RIS) and MS.

Methods: MTR data were acquired from 52 RIS, 201 relapsing–remitting MS (RRMS), 47 primary progressive MS (PPMS), and 43 control (CON) participants across four sites in the Canadian Prospective Cohort Study to Understand Progression in MS (CanProCo) using 3.0 T MRI systems. Mean MTR was compared between groups in whole cSC and sub-regions between C2-C4. Multiple linear regression was used to evaluate relationships between MTR and clinical outcomes, including the expanded disability status scale (EDSS), walking speed test (WST), and manual dexterity test (MDT).

Results: There were consistent group differences in MTR, which were most pronounced between PPMS and CON (−5.8% to −3.7%, $p \leq 0.01$). In PPMS, lower MTR was associated with greater disability as measured by EDSS ($\beta = -0.3$ to -0.1, $p \leq 0.03$), WST ($\beta = -0.9$ to -0.5, $p \leq 0.04$), and MDT ($\beta = -0.6$ and -0.5, $p = 0.04$). In RRMS, MTR was associated with only EDSS ($\beta = -0.1$, $p \leq 0.03$).

Interpretation: In this large sample of RIS and MS, cSC MTR was lowest in PPMS, with associations between MTR and clinical outcomes in MS but not RIS. These findings suggest that MTR provides important information about the underlying tissue microstructural integrity of the cSC relevant to clinical disability in established MS.

1 | Introduction

The spinal cord (SC) is a clinically eloquent structure commonly affected in multiple sclerosis (MS) and is highly relevant clinically, as the presence of disease-related tissue damage in the SC correlates with clinical dysfunction and is associated with worse clinical outcomes in early MS and radiologically isolated syndrome (RIS) [1–6]. As such, a non-invasive, quantitative in vivo assessment of the SC is of value to better understand how tissue microstructural changes contribute to clinical disability and disease progression in MS.

Prior studies using conventional MRI have demonstrated inconsistent relationships between SC lesion load and clinical disability [4, 7, 8]. Conversely, SC atrophy, as measured by upper cervical SC cross-sectional area (CSA), has shown stronger associations with clinical outcomes [7, 9–11]. However, SC atrophy represents irreversible tissue loss. Therefore, MRI measures that are sensitive to tissue microstructural changes prior to tissue destruction are of interest to prompt early intervention and delay or prevent disease progression [12].

One promising approach that can be applied to the SC in MS to evaluate tissue changes relevant to clinical disability is the magnetization transfer ratio (MTR). MTR is a semi-quantitative measure that reflects the exchange of magnetization between mobile (free) protons and immobile (restricted) protons bound to macromolecules such as myelin [13]. Thus, MTR provides an indirect estimate of myelin content, in addition to neuroaxonal integrity and water content, which may not be captured by conventional MRI alone [2]. In this study, we aimed to assess tissue microstructural abnormalities in the cervical SC using MTR and to evaluate its relationship with clinical outcome measures across MS subtypes. We hypothesized that people with primary progressive MS (PPMS), with more established disability, will exhibit greater tissue microstructural abnormalities, as measured by lower MTR in the cervical SC. Additionally, we hypothesized that these observed changes will associate more strongly with clinical outcome measures compared to people with RIS and relapsing–remitting MS (RRMS).

2 | Methods

2.1 | Participants

Participants were recruited from four collaborative sites as part of the Canadian prospective cohort study to understand progression in multiple sclerosis (CanProCo) between 2019 and 2022 [14]: St. Michael's Hospital (SMH), University of British Columbia (UBC), Centre Hospitalier de l'Université de Montréal (CHUM), and University of Alberta (UALB). People with RIS, clinically isolated syndrome (CIS) and MRI evidence of dissemination in space, RRMS and PPMS, and control participants (CON) were recruited. For the remainder of this manuscript, people with CIS and RRMS will be grouped together and referred to as the "RRMS subgroup". RIS and MS diagnoses were confirmed by the treating neurologist according to the 2009 Okuda and 2017 McDonald criteria, respectively [15, 16]. Inclusion criteria were as follows: ≥18 years of age and EDSS ≤6.5 for people with RIS and MS. People with RRMS were required to be within 5 years of disease onset and treatment naïve or not on disease-modifying therapy for ≥6 months. People with PPMS were required to be within 10 years of disease onset. Participants were excluded if they were human immunodeficiency virus positive or had been treated with chemotherapy for malignancy. Individuals with previous traumatic brain injury, brain surgery, recent cancer treatment, dementia, stroke, or functionally limiting neurological or psychiatric disease were excluded from the CON group. All individuals provided written informed consent. This study was approved by the Research Ethics Board at each institution (SMH: 18–325; UBC: H18-03047; CHUM: 2019–8085, 18.293-YP; UALB: Pro00086907).

2.2 | Clinical Assessments

The multiple sclerosis performance Test (MSPT), a self-administered, iPad-based system, is similar to the multiple sclerosis functional composite (MSFC) and was administered to people with RIS and MS [17–19]. The MSPT includes the walking speed test (WST) adapted from the timed 25-foot walk test (T25W) and the manual dexterity test (MDT) in the dominant hand adapted from the nine-hole peg test (9HPT) [17, 18]. The WST and MDT were selected as the clinical outcome measures in this study as walking speed and manual dexterity are both highly relevant to functional tracts in the SC. The traditional T25W and 9HPT were administered when the iPad-based MSPT was unavailable or based on participant preference. The expanded disability status scale (EDSS) score [20] was evaluated by Neurostatus-experienced neurologists.

2.3 | MRI Data Acquisition

MRI data were acquired on 3.0T systems (SMH: Siemens Magnetom Skyra, 20-channel head and neck coil, UBC: Philips Ingenia Elition, 16-channel head and neck coil, CHUM: Philips Ingenia, 16-channel head and neck coil, UALB: Siemens Prisma, 64-channel head and neck coil). The MR protocol was inspired by the spine-generic protocol [21]. MTR data were obtained in the upper cervical SC using a 3D gradient echo (GRE) sequence with (MT_{on}) and without (MT_{off}) an MT saturation pulse (Siemens: repetition time (TR) = 35 ms, echo time (TE) = 3.82 ms, flip angle (FA) = 9°, voxel size = 0.9 mm x 0.9 mm x 5.0 mm, 22 slices, acquisition time = 4 min 20s, 1200 Hz off-resonance Gaussian pulse, MT FA = 500°; Philips: TR = 57 ms, TE = 2.0 ms, FA = 9°, voxel size = 0.9 mm x 0.9 mm x 5.0 mm, 22 slices, acquisition time = 4 min 20s, 2200 Hz off-resonance single-lobe sinc-Gauss pulse, MT FA = 540°). T1-weighted data (MT-T1) were

also acquired with the MT saturation pulse absent (Siemens: TR = 15 ms, TE = 3.82 ms, FA = 15°, voxel size = 0.9 mm x 0.9 mm x 5.0 mm, 22 slices, acquisition time = 56 s; Philips: TR = 15 ms, TE = 2.0 ms, FA = 15°, voxel size = 0.9 mm x 0.9 mm x 5.0 mm, 22 slices, acquisition time = 34 s). A 3D T2-weighted sequence was acquired for vertebral labeling, tissue segmentation, image registration, and cervical SC CSA measurement (Siemens: TR = 1500 ms, TE = 120 ms, FA = 120°, voxel size = 0.8 mm x 0.8 mm x 0.8 mm, 64 slices, acquisition time = 4 min 2 s; Philips: TR = 3500 ms, TE = 120 ms, FA = 90°, voxel size = 0.8 mm x 0.8 mm x 0.8 mm, 63 slices, acquisition time = 5 min 11 s). MT scans were acquired in the axial plane, centered at the level of the C3/C4 intervertebral disc, and slices were aligned perpendicular to the longitudinal axis of the SC. For the post hoc, exploratory analyses, we acquired an additional SC phase-sensitive inversion recovery (PSIR) sequence (Siemens: TR = 2400 ms, TE = 9.4 ms, inversion time (TI) = 400 ms, FA = 120°, voxel size = 0.7 mm x 0.7 mm x 3.0 mm, 15 slices, acquisition time = 4 min 45 s; Philips: TR = 2400 ms, TE = 9.4 ms, TI = 400 ms, FA = 140°, voxel size = 0.7 mm x 0.7 mm x 3.0 mm, 16 slices, acquisition time = 4 min 48 s) and brain T1-weighted sequence (Siemens: TR = 1700 ms, TE = 2.12 ms, TI = 880 ms, FA = 10 °, voxel size = 1.0 mm x 1.0 mm x 1.0 mm, acquisition time = 3 min 37 s; Philips: TR = 8.3 ms, TE = 3.8 ms, TI = 1030 ms, turbo field echo (TFE) shot interval = 3000 ms, FA = 8 °, voxel size = 1.0 mm x 1.0 mm x 1.0 mm, acquisition time = 3 min 29 s).

2.4 | MRI Data Analysis

All analyses were performed using Spinal Cord Toolbox (https://spinalcordtoolbox.com) [22]. The SC was segmented using a convolutional neural network-based method (sct_deepseg_sc) [23] and vertebral levels were labeled on the T2-weighted images. Then, the T2-weighted images were registered to the PAM50 standard template space [24] to obtain the warp field, which was then used to transform the PAM50 template from standard to MT space for each participant. This ensured that the anatomical regions of interest (ROIs) defined in the PAM50 template were mapped to the corresponding region in the individual participant's MT space. MT_{on} and MT_{off} images were registered to MT-T1 space using slice-by-slice regularized registration [22]. MTR was computed in each voxel (sct_compute_mtr), which followed the equation: $MTR = [(MT_{off} - MT_{on})/MT_{off}]*100\%$. Mean MTR was computed in the following ROIs: whole SC, white matter (WM), gray matter (GM), dorsal columns (DC), lateral funiculi (LF), ventral funiculi (VF), and lateral corticospinal tracts (CST) averaged between cervical SC segments C2-C4 using the 'maximum a posteriori' method (Figure 1) [25]. These ROIs were selected a priori as they contain motor and sensory pathways highly relevant to clinical functions. The first and last three slices were excluded in the analysis for each individual to account for potential aliasing artifact in the furthest rostral or caudal slices of the imaging volume. Further, CSA was calculated between cervical SC segments C2-C4 (sct_process_segmentation). Data were inspected visually and removed or corrected when needed to ensure adequate image registration, absence of artifacts, and correct anatomical coverage. As a post hoc, exploratory analysis, we examined SC lesion pathology by repeating our analyses for normal-appearing SC ROIs, excluding visible lesions. Cervical SC lesions were manually segmented by a single rater on a PSIR sequence, which were then transformed into MT space for each participant. Mean MTR was computed in the normal-appearing SC ROIs. Additionally, the Canadian Brain Imaging Research Platform [26] was used to run FreeSurfer [27], which performed brain volume measurement based on brain T1-weighted images. Raw brain volumes were normalized to intracranial volume to adjust for variations in head size.

2.5 | Statistical Analysis

All statistical analyses were conducted using *R* software (https://www.r-project.org/). A chi-square test compared the sex distribution and one-way analysis of variance (ANOVA) compared age, disease duration, and clinical outcome measures across groups. A one-way analysis of covariance (ANCOVA) was used to test for group effects at each ROI, while controlling for age, sex, and MRI system vendor type. Tukey post hoc test for multiple comparisons was performed to compare MTR in each ROI between groups. Adjusted mean MTR was calculated using the estimated marginal means adjusted for co-variates. Relative percentage differences of the adjusted mean MTR between groups were calculated. To assess relationships between MTR and clinical outcome measures, multiple linear regression was utilized with MTR predicting clinical outcome measures separately for each ROI and patient group, adjusting for age, sex, and MRI system vendor type. *p*-values were adjusted for multiple testing using the false discovery rate (FDR) method. Adjusted $p < 0.05$ was considered significant. CSA analysis was performed using the same statistical methods. For the post hoc analysis examining the SC lesion pathology, *p*-values were not corrected for multiple testing given the exploratory nature of this analysis.

3 | Results

This cross-sectional study included 43 CON, 52 RIS, 201 RRMS, and 47 PPMS participants after removing MR data

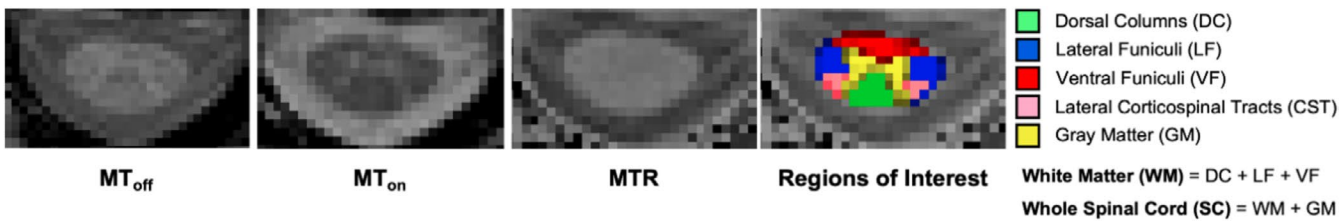

FIGURE 1 | Cervical spinal cord MT images of a study participant with PPMS. Regions of interest defined in the PAM50 standard template were mapped to each participant's MT space. Mean MTR was computed in the whole spinal cord, white matter, gray matter, dorsal columns, lateral funiculi, ventral funiculi, and lateral corticospinal tracts averaged between cervical spinal cord segments C2-C4.

from 3 RIS, 7 RRMS, and 2 PPMS participants due to imaging artifact or technical error. RIS participants were 79% female and had a mean age of 43 years (standard deviation (SD) = 10.9 years) with a mean disease duration of 2.2 years (SD = 2.7 years) and a median EDSS of 0.0 (range = 0.0–3.5). One RIS participant (1.9%) was on a disease-modifying therapy, minocycline. RRMS participants were 70% female and had a mean age of 36 years (SD = 10.0 years) with a mean disease duration of 0.7 years (SD = 1.2 years) and a median EDSS of 1.5 (range = 0.0–6.0). None of the RRMS participants were on disease-modifying therapy. PPMS participants were 49% female and had a mean age of 50 years (SD = 8.7 years) with a mean disease duration of 2.0 years (SD = 1.9 years) and a median EDSS of 4.0 (range = 1.5–6.5). A total of 49% of the PPMS participants were on ocrelizumab. CON participants were 65% female and had a mean age of 38 years (SD = 10.5 years). WST data from 2 RRMS and 1 PPMS, and MDT data from 2 RIS, 4 RRMS, and 1 PPMS participants were not captured or excluded due to technical errors, including an iPad device software issue, participants having difficulties using the iPad device or time constraints. Consequently, we ultimately used WST data from 52 people with RIS, 199 with RRMS, and 46 with PPMS, and MDT data from 50 with RIS, 197 with RRMS, and 46 with PPMS. Among these, 5 (9.6%) RIS, 51 (25.6%) RRMS, and 11 (23.9%) PPMS participants completed the T25W instead of WST. Five (10.0%) RIS, 51 (25.9%) RRMS, and 10 (21.7%) PPMS participants completed 9HPT instead of MDT. We observed significant group differences for sex, as well as age, disease duration, and clinical outcome measures ($p \leq 0.01$), which were not unexpected given the nature of the MS phenotypes. We included age, sex, and MRI system vendor type in our regression models to account for potential confounders. Table 1 lists the complete demographic and clinical characteristics of the participants, including disease-modifying therapy use and median WST and MDT.

There were significant differences in MTR between groups across all ROIs ($p \leq 0.02$). In PPMS, MTR was lower compared to CON in all cervical SC ROIs (relative percentage difference −5.8% to −3.7%, $p \leq 0.01$) even after controlling for age, sex, and MRI system vendor type (Figure 2). MTR was also lower in PPMS compared to RIS in most ROIs, including the whole SC, WM, LF, and CST (−3.3% to −2.6%, $p < 0.05$). There was no difference in MTR in any of the ROIs between PPMS and RRMS. Finally, when comparing RRMS to CON, MTR was lower in RRMS in most ROIs, including the whole SC, WM, DC, LF, and CST (−3.9% to −3.2%, $p \leq 0.001$) (Figure 2). CSA was lower in PPMS compared to RRMS (−5.5%, $p = 0.01$). CSA was also lower in PPMS compared to CON (−4.7%, $p = 0.16$) and RIS (−3.7%, $p = 0.30$), but these differences were not statistically significant.

When relationships were evaluated between MTR and clinical outcome measures in specific ROIs using multiple linear regression models adjusted for age, sex, and MRI system vendor type, there were associations between MTR and clinical outcome measures mostly in PPMS and to a lesser extent in RRMS (Tables 2 and 3). In general, MTR was most strongly associated with clinical outcome measures in the whole SC rather than specific regions in both RRMS and PPMS as measured by the largest beta coefficient. Specifically, in PPMS, there were consistent associations between MTR in nearly all ROIs and clinical outcome measures. Lower MTR was associated with greater EDSS ($\beta = -0.27$ to -0.14, $p \leq 0.03$) and WST ($\beta = -0.89$ to -0.54, $p \leq 0.04$) in all ROIs and with greater MDT in the DC and VF ($\beta = -0.61$ and -0.47, $p = 0.04$) (Table 3). Figure 3 illustrates adjusted associations between MTR and clinical outcome measures holding other co-variates constant in the whole SC of PPMS. The regression models evaluating relationships between cervical SC MTR and clinical outcomes in PPMS were able to explain up to 26% of the variance in EDSS, 29% of the variance in WST, and 14% of the variance in MDT (Table 3).

On the other hand, in RRMS, associations between MTR and clinical outcome measures were more limited. Relationships were observed between EDSS and MTR in all cervical SC ROIs, except VF ($\beta = -0.11$ to -0.07, $p \leq 0.03$) (Table 2). There were no significant associations observed in RRMS between MTR in cervical SC ROIs and WST or MDT. The regression models were able to explain up to 8% of the variance in EDSS in RRMS (Table 2). In RIS, there was no association between MTR and any of the clinical outcome measures.

When lesional tissue was removed, there were still group differences in MTR between CON and PPMS or RRMS across most SC ROIs ($p = 0.01$–0.08). Observed associations between MTR and clinical outcome measures were more limited; however, some key tracts still demonstrated expected relationships (Table S1).

There were no associations between CSA and clinical outcome measures, except for WST in RRMS ($\beta = -0.03$, $p = 0.03$), which was influenced by a single outlier (Table S2). Tables 2 and 3 present results from multiple linear regression analyses illustrating the associations between MTR and clinical outcome measures, with $p < 0.1$. All regression analyses, including those without significant relationships, are included in the Tables S2 and S3. In post hoc exploratory analyses, when normalized brain volume, adjusted for intracranial volume, was added to the multiple linear regression models, results remained similar (Table S4). Similarly, when disease duration (Table S5) or disease-modifying therapy (Table S6) for the PPMS subgroup was included, results remained similar.

4 | Discussion

In this study involving a large sample of people with early MS across the disease spectrum, we observed consistent group differences in cervical SC MTR, most pronounced between PPMS and CON. Lower MTR, indicative of reduced myelin, was associated with elevated clinical disability in PPMS and to a lesser extent in RRMS. In contrast, there were limited associations between CSA and clinical outcomes. These findings suggest that cervical SC MTR can detect subtle tissue microstructural changes relevant to clinical disability in people with early MS, prior to substantial tissue atrophy. Our results highlight that cervical SC MTR may be a useful paraclinical tool to measure disability worsening in early MS, which is a tremendous unmet need in the field.

TABLE 1 | Demographics, clinical, and MRI characteristics of study participants.

	CON	All patients	RIS	RRMS	PPMS	*p*
Participants, *n*	43	300	52	201	47	n/a
Female, *n* (%)	28 (65.1)	205 (68.3)	41 (78.8)	141 (70.1)	23 (48.9)	0.01
Mean Age, years (standard deviation, SD)	38 (10.5)	39 (11.2)	43 (10.9)	36 (10.0)	50 (8.7)	< 0.01
Mean Disease Duration, years (SD)	n/a	1.2 (1.8)	2.2 (2.7)	0.7 (1.2)	2.0 (1.9)	< 0.01
Median EDSS (range)	n/a	1.5 (0.0–6.5)	0.0 (0.0–3.5)	1.5 (0.0–6.0)	4.0 (1.5–6.5)	< 0.01
Median WST, seconds (range)	n/a	4.8 (3.0–26.2)	4.7 (3.4–8.1)	4.7 (3.0–14.8)	6.2 (3.5–26.2)	< 0.01
Median MDT, seconds (range)	n/a	22.7 (14.3–51.5)	22.6 (16.6–35.2)	22.2 (14.3–51.5)	25.4 (19.4–40.5)	< 0.01
Disease-Modifying Therapy, *n* (%)	n/a	24 (8.0)	1 (1.9)	0 (0.0)	23 (48.9)	n/a
Disease-Modifying Therapy Type	n/a	Minocycline, Ocrelizumab	Minocycline	n/a	Ocrelizumab	n/a
Adjusted mean CSA of the whole spinal cord, mm^2 (95% confidence interval (CI))	75.8 (73.5–78.1)	75.5 (74.5–76.4)	75.0 (72.8–77.2)	76.4 (75.3–77.6)	72.2 (69.9–74.6)	0.03
Adjusted mean MTR of the whole spinal cord, % (95% CI)	48.9 (48.2–49.6)	47.3 (47.0–47.5)	47.7 (47.1–48.4)	47.3 (47.0–47.7)	46.5 (45.8–47.2)	< 0.01
Adjusted mean MTR of the white matter, % (95% CI)	49.7 (49.0–50.4)	47.8 (47.6–48.1)	48.4 (47.7–49.1)	47.9 (47.6–48.3)	47.0 (46.3–47.8)	< 0.01
Adjusted mean MTR of the gray matter, % (95% CI)	46.4 (45.7–47.1)	45.4 (45.1–45.7)	45.6 (45.0–46.3)	45.5 (45.1–45.9)	44.7 (44.0–45.5)	0.02
Adjusted mean MTR of the dorsal columns, % (95% CI)	49.4 (48.6–50.3)	47.5 (47.2–47.9)	48.0 (47.1–48.8)	47.6 (47.1–48.0)	47.0 (46.2–47.9)	< 0.01
Adjusted mean MTR of the lateral funiculi, % (95% CI)	49.8 (49.0–50.6)	47.9 (47.6–48.2)	48.5 (47.8–49.2)	48.0 (47.6–48.3)	46.9 (46.1–47.7)	< 0.01
Adjusted mean MTR of the ventral funiculi, % (95% CI)	49.8 (48.8–50.8)	48.2 (47.8–48.6)	48.8 (47.8–49.8)	48.4 (47.9–48.9)	47.2 (46.1–48.2)	< 0.01
Adjusted mean MTR of the corticospinal tracts, % (95% CI)	48.5 (47.7–49.3)	46.5 (46.2–46.8)	47.3 (46.5–48.0)	46.5 (46.1–46.9)	45.7 (44.9–46.6)	< 0.01

Note: Adjusted means represent the estimated marginal means adjusted for the effects of co-variates (age, sex, and MRI system vendor type) using the 'emmeans' package in R. Disease duration was defined as the time since diagnosis. *p* values were derived using a chi-square test for sex, ANOVA for age, disease duration and clinical outcome measures, and ANCOVA for CSA and MTR of SC ROIs with *p*-values adjusted for multiple testing using the false discovery rate method.

Although the cervical SC is known to be highly relevant to clinical disability in MS, it has been understudied using quantitative MRI techniques due to technical challenges [28]. Recent advances, including standardized acquisition protocols and semi-automated analysis tools, including the Spinal Cord Toolbox, have enabled quantitative SC MRI with clinically feasible acquisition times and quality [21, 22, 29].

Among quantitative MRI techniques, we chose MT imaging as it utilizes a widely available pulse sequence, has a relatively rapid acquisition time, and requires simple post-processing. MT imaging is also one of the few quantitative MRI techniques that have been used in contemporary clinical trials for MS and has demonstrated treatment effects and relationships with clinical disability, suggesting that MT imaging is a practically feasible technique with clinical relevance that may eventually have clinical utility in individual patients [29–31]. Additionally, MT imaging can detect early tissue changes prior to substantial atrophy, making it useful in clinical trials and practice to evaluate treatment response and monitor disease worsening. While MTR is sensitive to myelin [32–35], it can also be affected by axonal density, edema, and inflammation [36–38] as well as MT pulse characteristics, MRI system vendor, and field strength [28].

Despite these limitations, MTR has been shown to be reliable in the SC [39] and prior studies using MT imaging in smaller samples have consistently demonstrated its ability to detect tissue microstructural abnormalities in MS [40–46]. Cervical SC MTR has been reported to be lower in MS compared to CON [40–43] and has been associated with clinical disability, including EDSS, T25W, and 9HPT [41, 43, 45, 46], supporting

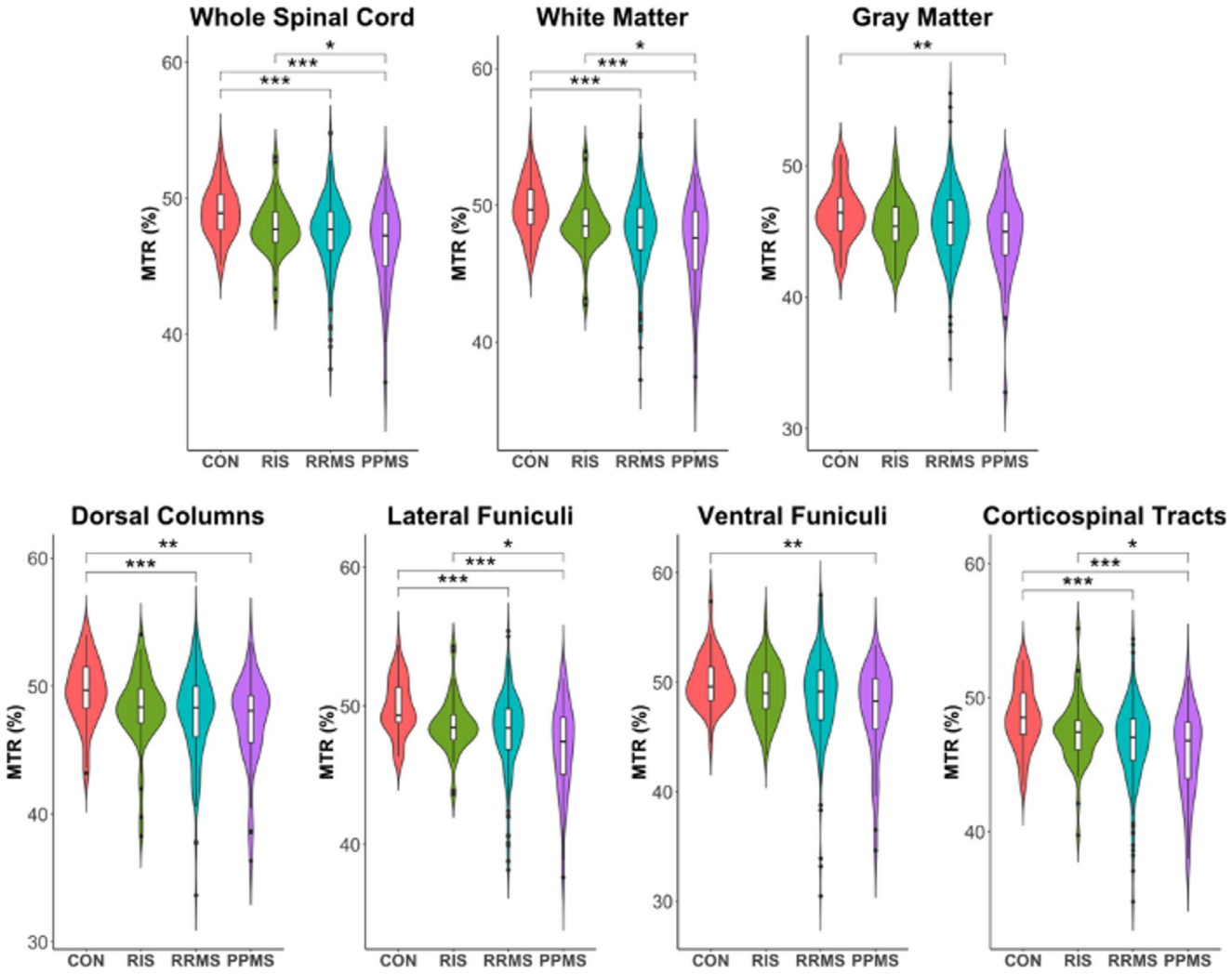

FIGURE 2 | Mean MTR comparisons between CON, RIS, RRMS, and PPMS in the whole spinal cord, white matter, gray matter, dorsal columns, lateral funiculi, ventral funiculi and lateral corticospinal tracts averaged between cervical spinal cord segments C2-C4. *$p = 0.01–0.05$; **$p = 0.001–0.01$; ***$p < 0.001$.

TABLE 2 | Relationships between MTR and clinical outcome measures in multiple linear regression models for RRMS with adjusted $p < 0.1$.

Clinical outcome	Region of interest	Regression coefficient (β)	95% CI	p*	R^2
EDSS	Whole Spinal Cord	−0.11	−0.18, −0.05	**0.01**	0.08
	White Matter	−0.10	−0.16, −0.04	**0.01**	0.08
	Gray Matter	−0.09	−0.15, −0.03	**0.02**	0.07
	Dorsal Columns	−0.07	−0.13, −0.02	**0.02**	0.06
	Lateral Funiculi	−0.11	−0.16, −0.05	**0.01**	0.08
	Corticospinal Tracts	−0.07	−0.13, −0.02	**0.03**	0.06

*p values were adjusted for multiple testing using the false discovery rate method. Significant adjusted p values are bolded.

our findings. Combès et al. [42] observed minimal correlation between cervical SC MTR and clinical disability in people with recently diagnosed RRMS who had a low range of disability, which aligns with our findings that cervical SC MTR demonstrated less pronounced associations with clinical outcomes in people with early RRMS, who were also recently diagnosed (typically within < 1 year) with limited variation in disability levels, compared to those with PPMS. Additionally, prior studies have shown that cervical SC MTR abnormalities can be detected even in the absence of substantial SC atrophy, particularly in early MS, further supporting our results [42, 44]. Lee et al. [47] utilized an alternative myelin MRI measure, myelin heterogeneity index (MHI) derived from myelin water imaging and found differences in cervical SC MHI between progressive MS and both RRMS and CON, and correlations were observed with EDSS and 9HPT. While evidence

TABLE 3 | Relationships between MTR and clinical outcome measures in multiple linear regression models for PPMS with adjusted $p < 0.1$.

Clinical outcome	Region of interest	Regression coefficient (β)	95% CI	p*	R^2
EDSS	Whole Spinal Cord	−0.27	−0.42, −0.12	**< 0.01**	0.25
	White Matter	−0.27	−0.41, −0.12	**< 0.01**	0.26
	Gray Matter	−0.19	−0.34, −0.04	**0.02**	0.15
	Dorsal Columns	−0.22	−0.35, −0.09	**0.01**	0.22
	Lateral Funiculi	−0.25	−0.39, −0.11	**< 0.01**	0.25
	Ventral Funiculi	−0.14	−0.26, −0.02	**0.03**	0.13
	Corticospinal Tracts	−0.23	−0.37, −0.08	**0.01**	0.20
WST	Whole Spinal Cord	−0.89	−1.42, −0.37	**0.01**	0.24
	White Matter	−0.83	−1.34, −0.33	**0.01**	0.24
	Gray Matter	−0.76	−1.27, −0.26	**0.01**	0.21
	Dorsal Columns	−0.54	−1.04, −0.05	**0.04**	0.13
	Lateral Funiculi	−0.75	−1.25, −0.26	**0.01**	0.21
	Ventral Funiculi	−0.72	−1.09, −0.35	**< 0.01**	0.29
	Corticospinal Tracts	−0.63	−1.14, −0.12	**0.03**	0.16
MDT	Whole Spinal Cord	−0.56	−1.15, 0.03	0.07	0.10
	White Matter	−0.59	−1.16, −0.02	0.05	0.12
	Dorsal Columns	−0.61	−1.14, −0.08	**0.04**	0.14
	Ventral Funiculi	−0.47	−0.88, −0.06	**0.04**	0.14

*p values were adjusted for multiple testing using the false discovery rate method. Significant adjusted p values are bolded.

for cervical SC MTR differences in RIS is more limited, we previously reported that, across a wide range of quantitative MRI measures, only cervical SC MTR showed a trend of difference between RIS and CON in a small sample size [48].

Our findings expand upon prior studies by including a large sample of participants early in the disease course and evaluating both whole SC and specific functional SC regions. This approach enabled us to evaluate both global and functionally distinct cervical SC regions in relation to multiple clinical outcomes, including EDSS and iPad-based WST and MDT. A key advantage of the digital assessments is their accessibility, as they can be conducted not only in clinical settings but also at home, making it useful for people with greater disability or those living in rural and underserved areas. Additionally, digital assessments can help address time constraints in clinical practice, making them more feasible for routine use and enabling better monitoring of clinical worsening over time. By including people with RIS, early RRMS, and early PPMS, our study examined MTR differences across a spectrum of MS. Furthermore, our study utilized data collected across 4 sites and 2 major MRI system vendors using 3T MRI systems, improving the generalizability of our findings. Notably, MTR of the whole SC, rather than specific regions, was most robustly associated with clinical outcomes, despite expectations that specific functional columns would show stronger associations. This likely reflects the technical challenges of imaging the SC and accurately localizing specific functional columns. Thus, our results suggest that, for practical reasons, it may be sufficient and most reliable to extract quantitative measures from the whole SC rather than smaller, column-specific ROIs in clinical trials and practice.

In PPMS, lower MTR was associated with greater EDSS and WST across all ROIs and with MDT in DC and VF, with trends noted in the whole SC and WM. The more limited associations observed with MDT are likely related to the functional organization of the SC and that manual dexterity may be more relevant to sensory functions, which are mediated by the DC and spinothalamic tracts located in the DC and VF. We also found that, in RRMS, lower MTR was associated with greater EDSS, but not WST or MDT across all ROIs except VF. One possible reason is that we included people very early on in the disease course of RRMS—most were newly diagnosed with a mean disease duration of less than 1 year and a median EDSS of 1.5. Given the limited variation in disability levels and early stages of MS in our RRMS cohort, it is possible that only the global disability measure may have been sufficiently impaired to demonstrate associations with MTR. A composite limb function score using WST and MDT also showed no relationship with MTR in RRMS. There were no associations between MTR and any of the clinical outcome measures in RIS, which is not unexpected as RIS describes people without overt clinical symptoms of MS.

In an exploratory analysis excluding visible lesions, we observed more limited but clear differences between MS subtypes and its relationship to clinical outcome measures. These findings are not surprising, since the lesional tissue represents the most damaged areas and unlike the brain, where lesions may occupy

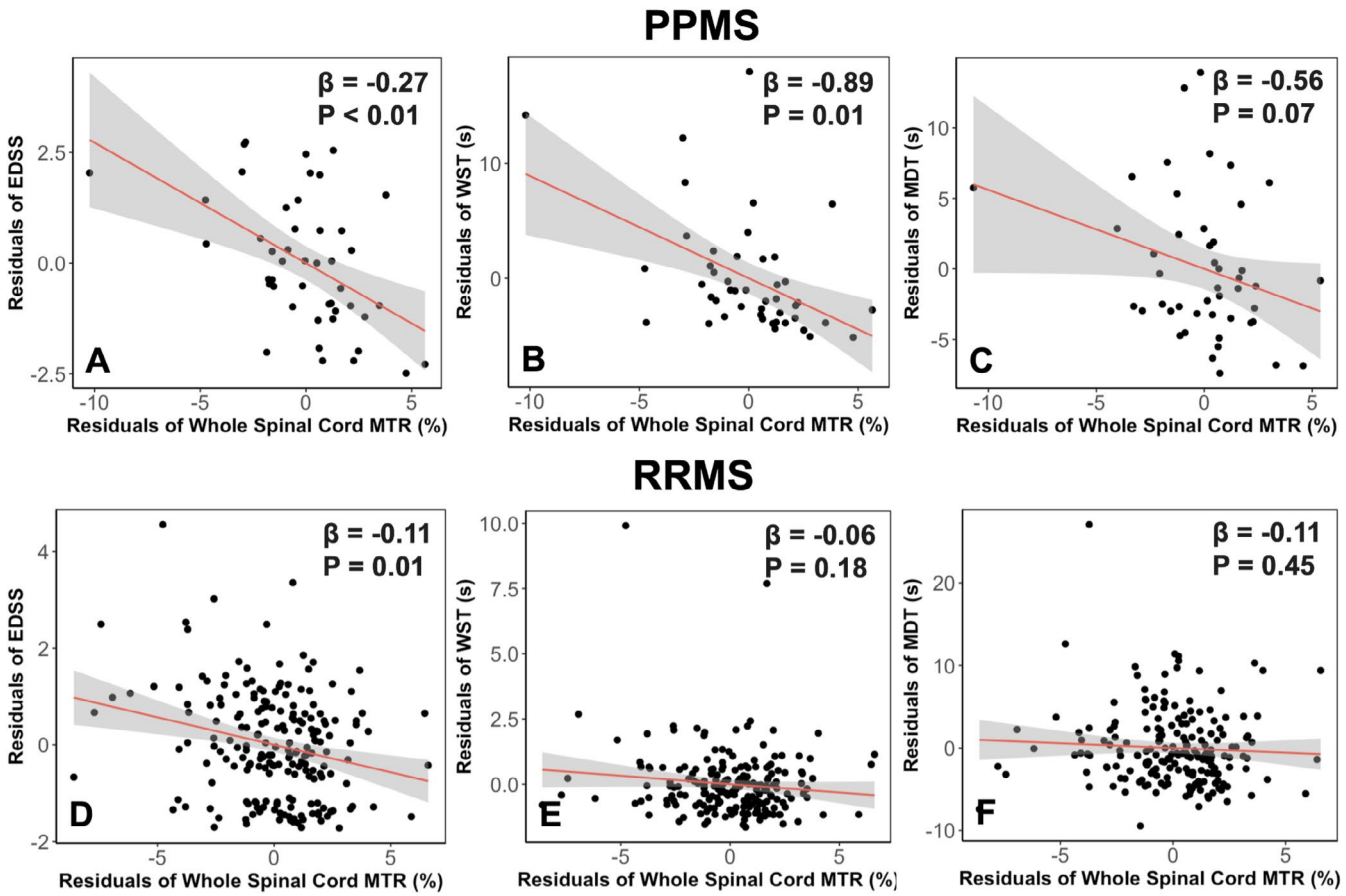

FIGURE 3 | Partial regression (added variable) plots of adjusted relationships between the whole spinal cord MTR and (A for PPMS, D for RRMS) EDSS score, (B for PPMS, E for RRMS) WST time, and (C for PPMS, F for RRMS) MDT time adjusted for age, sex, and MRI system vendor type in multiple linear regression models.

only a small volume relative to the whole brain, in the cervical SC, lesions can occupy the majority of the cervical SC, resulting in substantial MR data loss related to MS-related damage. Therefore, it is understandable that the strength of the relationships would be weaker. Yet, the fact that we were still able to observe differences between MS subtypes in non-lesional tissue MTR and relationships with clinical outcome measures highlights the relevance of both lesional and non-lesional tissue in the cervical SC.

Of note, there were no associations between CSA and clinical outcome measures, except for WST in RRMS, influenced by a single outlier. This contrasts with findings from several smaller studies [9, 12, 45] likely because we included people early in the disease course before substantial cervical SC atrophy occurred. In support of this, we observed an adjusted mean CSA of 72.2mm^2 in 47 PPMS participants (mean disease duration = 2 years, median EDSS = 4.0), which was higher than the mean CSA reported in previous studies. Our group previously found a mean CSA of 67.2mm^2 between C3-C4 in 30 progressive MS participants (mean disease duration = 11 years, mean EDSS = 6.0) [12] and a meta-analysis found a pooled mean cervical SC CSA of 71.0mm^2 for PPMS [49]. Further, in the present study, we likely did not observe many associations between SC CSA and the clinical outcome measures in RRMS because they had a relatively short disease duration and minimal disability (mean disease duration = 0.7 years, median EDSS = 1.5).

Notably, our data were collected from four sites using 3.0 T MRI systems from two different MRI system vendors. Despite this, we found robust associations between MTR and clinical outcome measures in established MS, suggesting that obtaining quantitative measures such as MTR in the SC is feasible in multi-centre settings. This is an encouraging outcome when considering MRI measures that may be useful in clinical trials and practice.

There are several limitations to our study. First, we only examined the upper cervical SC; thus, upstream or downstream pathology was not considered. Despite this, we demonstrated robust MTR associations, suggesting that the cervical SC alone is relevant to clinical disability. Indeed, prior studies found that SC damage is most often found in the upper cervical SC [2, 50, 51]. Imaging the lower SC is challenging due to the lack of dedicated hardware and artifacts from magnetic field inhomogeneity. Second, while it would have been ideal for all participants to complete the iPad-based tests, a small proportion of participants underwent traditional tests. However, we found no significant differences between T25W and WST or 9HPT and MDT, so they were grouped together in our analyses. Third, small ROIs (e.g., VF, CST) may be prone to partial volume effects; therefore, these results should be interpreted with caution. Fourth, our study only evaluated MTR, which captures a portion of SC microstructural changes. Future studies should include other quantitative MRI techniques, such as diffusion MRI, susceptibility weighted imaging, and other myelin-sensitive imaging techniques, to

provide deeper insights into additional pathological processes contributing to clinical disability in MS [29]. Fifth, while nearly half of PPMS participants were on ocrelizumab, none of the RRMS participants were on disease-modifying therapies, which may have influenced the comparison of SC MTR and its relationship to clinical disability. However, including treatment as a co-variate in the regression model for PPMS did not alter the results. Sixth, the relatively modest associations between SC MTR and clinical outcomes in RRMS and RIS may reflect the limitations of the clinical measures used. It is possible that more sensitive measures (e.g., posturography, vibration sense test, and six-minute walk test) could better detect subtle disability and strengthen the association with SC MTR in early MS and RIS. Finally, our findings should be interpreted in the context of current clinical MS subtypes, which, while commonly used in clinical practice, are not biologically defined. Moreover, there is a growing consensus that disease progression begins early in the disease course.

In conclusion, in this large, multi-centre and multi-vendor study of people with early MS, we found robust associations between cervical SC MTR and clinical outcomes, particularly in PPMS. Notably, whole SC MTR was most robustly associated with clinical disability, suggesting that segmenting the cervical SC into functional columns may not be necessary in clinical trials or practice. Our findings support MT imaging as a viable technique for assessing tissue microstructural abnormalities relevant to clinical disability across the MS spectrum, especially early in the disease course when SC atrophy may not be as strongly associated with clinical outcomes. With longitudinal validation in external cohorts, particularly those reflecting a wider range of people with MS including those with longer disease durations, our findings set the stage for developing cervical SC MTR as a promising tool to evaluate treatment effects and monitor disability worsening in clinical trials and practice.

Author Contributions

L.E.L., S.J.G., M.H., A.F., T.A.S., J.O. contributed to the conception and design of the study. L.E.L., J.C., I.M.V., K.S., N.R.-R., N.C., A.C., A.A., and P.-L.B. contributed to the analysis of data. M.G., A.T., N.A., F.G., L.D.L., S.B.P., A.P., A.S., P.S., R.T., Y.Z., S.K. contributed to the acquisition of data. All authors contributed to the interpretation of the data and approved the final version of the manuscript.

Acknowledgments

We sincerely thank all study participants, CanProCo Executive Board Committee and collaborators. We also thank Dr. Rosane Nisenbaum, Dr. Enedino Hernandez-Torres, Dr. Shelly Au, Michelle Chen, Molly Hyde, Marc Khoury, Gina D'Souza, Erin Gallinger, Fasna Raufdeen, Elaine Roger, Kyra West, Sara Tipnis, Pamala Dupont, Leah White, Katerina Downing, and Aman Sharma for their guidance and contributions. This study was funded by MS Canada, Biogen Canada, Brain Canada Foundation, Hoffmann-La Roche Limited, and Government of Alberta.

Conflicts of Interest

Lisa Eunyoung Lee, Julien Cohen-Adad, Irene Vavasour, Melanie Guenette, Katherine Sawicka, Neda Rashidi-Ranjbar, Nathan Churchill, Akash Chopra, Adelia Adelia, Pierre-Louis Benveniste, Nathalie Arbour, Scott B. Patten, Alexandre Prat, Alice Schabas, Roger Tam, Yunyan Zhang, Simon J. Graham, and Tom A. Schweizer report no conflicts of interest relevant to this study. Anthony Traboulsee is the MS Canada Research Chair at the University of British Columbia. Fabrizio Giuliani received speaker fees, research support, travel support, or fees for serving on advisory boards by MS Canada, National MS Society, Canadian Institute of Health Research, Biogen, Merck, Novartis, Roche, and Sanofi. Larry Lynd has received grant-funding from Pfizer Canada for research unrelated to multiple sclerosis. Penelope Smyth received speaking honoraria and honoraria from serving on the scientific advisory boards of: Biogen-Idec Pharmaceuticals, Roche Pharmaceuticals, EMD Serono Canada Pharmaceuticals, Novartis Pharmaceuticals, and honoraria for serving as an expert reviewer for the Short Term Exceptional Drug Therapy program in Alberta, Canada. She is a co-investigator in receiving an unrestricted research grant for a prospective pregnancy registry cohort project in Canada from Biogen-Idec Canada. Mojgan Hodaie received support from NIH as co-investigator in projects that focus on neuroimaging. Anthony Feinstein received grant support from MS Canada and the MacArthur and Knight Foundations. He has book royalties from Johns Hopkins University Press, G Editions, and Cambridge University Press. He received speaking honoraria from Novartis and Merck-Serono. Shannon Kolind received consulting fees from Abbvie and has received research support from Roche, Sanofi-Genzyme and Biogen. Jiwon Oh is supported by the Waugh Family Chair in MS Research at the University of Toronto and the Barford and Love MS Fund of the St. Michael's Hospital Foundation and has received research funding from Biogen-Idec, Eli-Lilly, EMD Serono, Novartis, Roche, and Sanofi-Genzyme.

Data Availability Statement

Anonymized data will be shared upon request from qualified investigators who have appropriate data-sharing agreements in place.

References

1. J. Bot, F. Barkhof, H. Polman, et al., "Spinal Cord Abnormalities in Recently Diagnosed MS Patients: Added Value of Spinal MRI Examination," *Neurology* 62 (2004): 226–233.

2. M. Moccia, S. Ruggieri, A. Ianniello, A. Toosy, C. Pozzilli, and O. Ciccarelli, "Advances in Spinal Cord Imaging in Multiple Sclerosis," *Therapeutic Advances in Neurological Disorders* 12 (2019): 1756286419840593.

3. W. J. Brownlee, D. R. Altmann, F. Prados, et al., "Early Imaging Predictors of Long-Term Outcomes in Relapse-Onset Multiple Sclerosis," *Brain* 142 (2019): 2276–2287.

4. G. Lycklama à Nijeholt, F. Barkhof, P. Scheltens, et al., "MR of the Spinal Cord in Multiple Sclerosis: Relation to Clinical Subtype and Disability," *American Journal of Neuroradiology* 18, no. 6 (1997): 1041–1048.

5. D. T. Okuda, E. M. Mowry, B. A. C. Cree, et al., "Asymptomatic Spinal Cord Lesions Predict Disease Progression in Radiologically Isolated Syndrome," *Neurology* 76, no. 8 (2011): 686–692.

6. M. H. Sombekke, M. P. Wattjes, L. J. Balk, et al., "Spinal Cord Lesions in Patients With Clinically Isolated Syndrome: A Powerful Tool in Diagnosis and Prognosis," *Neurology* 80 (2013): 69–75.

7. F. Barkhof, "The Clinico-Radiological Paradox in Multiple Sclerosis Revisited," *Current Opinion in Neurology* 15 (2002): 239–245.

8. G. Nijeholt, M. A. van Walderveen, J. A. Castelijns, et al., "Brain and Spinal Cord Abnormalities in Multiple Sclerosis. Correlation Between MRI Parameters, Clinical Subtypes and Symptoms," *Brain* 121 (1998): 687–697.

9. F. X. Aymerich, C. Auger, J. Alonso, et al., "Cervical Cord Atrophy and Long-Term Disease Progression in Patients With Primary-Progressive Multiple Sclerosis," *American Journal of Neuroradiology* 39 (2018): 399–404.

10. M. A. Rocca, M. A. Horsfield, S. Sala, et al., "A Multicenter Assessment of Cervical Cord Atrophy Among MS Clinical Phenotypes," *Neurology* 76 (2011): 2096–2102.

11. C. Lukas, M. H. Sombekke, B. Bellenberg, et al., "Relevance of Spinal Cord Abnormalities to Clinical Disability in Multiple Sclerosis: MR Imaging Findings in a Large Cohort of Patients," *Radiology* 269 (2013): 542–552.

12. J. Oh, M. Chen, K. Cybulsky, et al., "Five-Year Longitudinal Changes in Quantitative Spinal Cord MRI in Multiple Sclerosis," *Multiple Sclerosis* 27 (2021): 549–558.

13. R. M. Henkelman, G. J. Stanisz, and S. J. Graham, "Magnetization Transfer in MRI: A Review," *NMR in Biomedicine* 14 (2001): 57–64.

14. J. Oh, N. Arbour, F. Giuliani, et al., "The Canadian Prospective Cohort Study to Understand Progression in Multiple Sclerosis (CanProCo): Rationale, Aims, and Study Design," *BMC Neurology* 21, no. 1 (2021): 418.

15. D. T. Okuda, E. M. Mowry, A. Beheshtian, et al., "Incidental MRI Anomalies Suggestive of Multiple Sclerosis: The Radiologically Isolated Syndrome," *Neurology* 72 (2009): 800–805.

16. A. J. Thompson, B. L. Banwell, F. Barkhof, et al., "Diagnosis of Multiple Sclerosis: 2017 Revisions of the McDonald Criteria," *Lancet Neurology* 17 (2018): 162–173.

17. J. K. Rhodes, D. Schindler, S. M. Rao, et al., "Multiple Sclerosis Performance Test: Technical Development and Usability," *Advanced Therapy* 36 (2019): 1741–1755.

18. S. M. Rao, R. Galioto, M. Sokolowski, et al., "Multiple Sclerosis Performance Test: Validation of Self-Administered Neuroperformance Modules," *European Journal of Neurology* 27 (2020): 878–886.

19. D. Ontaneda, N. LaRocca, T. Coetzee, R. Rudick, and NMSS MSFC Task Force, "Revisiting the Multiple Sclerosis Functional Composite: Proceedings From the National Multiple Sclerosis Society (NMSS) Task Force on Clinical Disability Measures," *Multiple Sclerosis* 18 (2012): 1074–1080.

20. J. F. Kurtzke, "Rating Neurologic Impairment in Multiple Sclerosis: An Expanded Disability Status Scale (EDSS)," *Neurology* 33 (1983): 1444–1452.

21. J. Cohen-Adad, E. Alonso-Ortiz, M. Abramovic, et al., "Generic Acquisition Protocol for Quantitative MRI of the Spinal Cord," *Nature Protocols* 16 (2021): 4611–4632.

22. B. De Leener, S. Lévy, S. M. Dupont, et al., "SCT: Spinal Cord Toolbox, an Open-Source Software for Processing Spinal Cord MRI Data," *NeuroImage* 145 (2017): 24–43.

23. C. Gros, B. De Leener, A. Badji, et al., "Automatic Segmentation of the Spinal Cord and Intramedullary Multiple Sclerosis Lesions With Convolutional Neural Networks," *NeuroImage* 184 (2019): 901–915.

24. B. De Leener, V. S. Fonov, D. L. Collins, V. Callot, N. Stikov, and J. Cohen-Adad, "PAM50: Unbiased Multimodal Template of the Brainstem and Spinal Cord Aligned With the ICBM152 Space," *NeuroImage* 165 (2018): 170–179.

25. S. Lévy, M. Benhamou, C. Naaman, P. Rainville, V. Callot, and J. Cohen-Adad, "White Matter Atlas of the Human Spinal Cord With Estimation of Partial Volume Effect," *NeuroImage* 119 (2015): 262–271.

26. T. Sherif, P. Rioux, M. Rousseau, et al., "CBRAIN: A Web-Based, Distributed Computing Platform for Collaborative Neuroimaging Research," *Frontiers in Neuroinformatics* 8 (2014): 54.

27. B. Fischl, "FreeSurfer," *NeuroImage* 62 (2012): 774–781.

28. P. W. Stroman, C. Wheeler-Kingshott, M. Bacon, et al., "The Current State-Of-The-Art of Spinal Cord Imaging: Methods," *NeuroImage* 84 (2014): 1070–1081.

29. A. J. E. Combes, M. A. Clarke, K. P. O'Grady, K. G. Schilling, and S. A. Smith, "Advanced Spinal Cord MRI in Multiple Sclerosis: Current Techniques and Future Directions," *NeuroImage: Clinical* 36 (2022): 103244.

30. C. Granziera, J. Wuerfel, F. Barkhof, et al., "Quantitative Magnetic Resonance Imaging Towards Clinical Application in Multiple Sclerosis," *Brain* 144 (2021): 1296–1311.

31. J. Oh, D. Ontaneda, C. Azevedo, et al., "Imaging Outcome Measures of Neuroprotection and Repair in MS: A Consensus Statement From NAIMS," *Neurology* 92 (2019): 519–533.

32. J. T. Chen, D. L. Collins, H. L. Atkins, M. S. Freedman, D. L. Arnold, and Canadian MS/BMT Study Group, "Magnetization Transfer Ratio Evolution With Demyelination and Remyelination in Multiple Sclerosis Lesions," *Annals of Neurology* 63 (2008): 254–262.

33. J. Bot, E. Blezer, W. Kamphorst, et al., "The Spinal Cord in Multiple Sclerosis: Relationship of High-Spatial-Resolution Quantitative MR Imaging Findings to Histopathologic Results," *Radiology* 233 (2004): 531–540.

34. K. Schmierer, F. Scaravilli, D. R. Altmann, G. J. Barker, and D. H. Miller, "Magnetization Transfer Ratio and Myelin in Postmortem Multiple Sclerosis Brain," *Annals of Neurology* 56 (2004): 407–415.

35. M. S. Deloire-Grassin, B. Brochet, B. Quesson, et al., "In Vivo Evaluation of Remyelination in Rat Brain by Magnetization Transfer Imaging," *Journal of the Neurological Sciences* 178 (2000): 10–16.

36. I. M. Vavasour, C. Laule, D. K. B. Li, A. L. Traboulsee, and A. L. MacKay, "Is the Magnetization Transfer Ratio a Marker for Myelin in Multiple Sclerosis?," *Journal of Magnetic Resonance Imaging* 33 (2011): 713–718.

37. J. H. Van Waesberghe, W. Kamphorst, C. J. De Groot, et al., "Axonal Loss in Multiple Sclerosis Lesions: Magnetic Resonance Imaging Insights Into Substrates of Disability," *Annals of Neurology* 46 (1999): 747–754.

38. J. P. Mottershead, K. Schmierer, M. Clemence, et al., "High Field MRI Correlates of Myelin Content and Axonal Density in Multiple Sclerosis - a Post-Mortem Study of the Spinal Cord," *Journal of Neurology* 250 (2003): 1293–1301.

39. S. Lévy, M. Guertin, A. Khatibi, et al., "Test-Retest Reliability of Myelin Imaging in the Human Spinal Cord: Measurement Errors Versus Region- and Aging-Induced Variations," *PLoS One* 13 (2018): e0189944.

40. N. Silver, G. Barker, N. Losseff, et al., "Magnetisation Transfer Ratio Measurement in the Cervical Spinal Cord: A Preliminary Study in Multiple Sclerosis," *Neuroradiology* 39 (1997): 441–445.

41. G. Lycklama à Nijeholt, J. Castelijns, R. Lazeron, et al., "Magnetization Transfer Ratio of the Spinal Cord in Multiple Sclerosis: Relationship to Atrophy and Neurological Disability," *Journal of Neuroimaging* 10 (2000): 67–72.

42. B. Combès, A. Kerbrat, J. Ferré, et al., "Focal and Diffuse Cervical Spinal Cord Damage in Patients With Early Relapsing-Remitting MS: A Multicentre Magnetisation Transfer Ratio Study," *Multiple Sclerosis Journal* 25 (2019): 1113–1123.

43. M. Filippi, M. Bozzali, M. Horsfield, et al., "A Conventional and Magnetization Transfer MRI Study of the Cervical Cord in Patients With MS," *Neurology* 54 (2000): 207–213.

44. H. Kearney, M. C. Yiannakas, R. S. Samson, C. A. M. Wheeler-Kingshott, O. Ciccarelli, and D. H. Miller, "Investigation of Magnetization Transfer Ratio-Derived Pial and Subpial Abnormalities in the Multiple Sclerosis Spinal Cord," *Brain* 137 (2014): 2456–2468.

45. J. Oh, K. Zackowski, M. Chen, et al., "Multiparametric MRI Correlates of Sensorimotor Function in the Spinal Cord in Multiple Sclerosis," *Multiple Sclerosis* 19 (2013): 427–435.

46. K. M. Zackowski, S. A. Smith, D. S. Reich, et al., "Sensorimotor Dysfunction in Multiple Sclerosis and Column-Specific Magnetization Transfer-Imaging Abnormalities in the Spinal Cord," *Brain* 132 (2009): 1200–1209.

47. L. E. Lee, I. M. Vavasour, A. Dvorak, et al., "Cervical Cord Myelin Abnormality Is Associated With Clinical Disability in Multiple Sclerosis," *Multiple Sclerosis (Houndmills)* 27 (2021): 2191–2198.

48. P. Alcaide-Leon, K. Cybulsky, S. Sankar, et al., "Quantitative Spinal Cord MRI in Radiologically Isolated Syndrome," *Neurology Neuroimmunology & Neuroinflammation* 5 (2018): e436.

49. C. Casserly, E. E. Seyman, P. Alcaide-Leon, et al., "Spinal Cord Atrophy in Multiple Sclerosis: A Systematic Review and Meta-Analysis," *Journal of Neuroimaging* 28 (2018): 556–586.

50. K. Weier, J. Mazraeh, Y. Naegelin, et al., "Biplanar MRI for the Assessment of the Spinal Cord in Multiple Sclerosis," *Multiple Sclerosis* 18 (2012): 1560–1569.

51. D. Eden, C. Gros, A. Badji, et al., "Spatial Distribution of Multiple Sclerosis Lesions in the Cervical Spinal Cord," *Brain* 142 (2019): 633–646.

Supporting Information

Additional supporting information can be found online in the Supporting Information section.